치의과학박사 학위논문

Analysis of fractal dimension and degree of anisotropy to differentiate osteosarcoma from osteomyelitis on panoramic radiographs

파노라마방사선영상에서 골육종과 골수염의 감별을 위한 프랙탈 차원과 비등방성 분석

2023년 2월

서울대학교 치의학대학원

치의과학과 영상치의학 전공

정 지 훈

Analysis of fractal dimension and degree of anisotropy to differentiate osteosarcoma from osteomyelitis on panoramic radiographs

지도교수 허 경 회

이 논문을 치의과학 박사학위논문으로 제출함

2022년 11월

서울대학교 치의학대학원

치의과학과 영상치의학 전공

정 지 훈

정지훈의 치의과학 박사학위논문을 인준함

2023년 1월

위 원 장 ______________________ (인)

부위원장 ______________________ (인)

위 원 ______________________ (인)

위 원 ______________________ (인)

위 원 ______________________ (인)

-ABSTRACT-

Analysis of fractal dimension and degree of anisotropy to differentiate osteosarcoma from osteomyelitis on panoramic radiographs

Jihun Jung, DDS, MSD

Department of Oral and Maxillofacial Radiology, Graduate School,

Seoul National University

(Directed by Professor Kyung-Hoe Huh, DDS, MSD, PhD)

Purpose: It is difficult to diagnose osteosarcoma (OS) at an early stage in dentistry, and it is easy to misdiagnose because OS looks similar to osteomyelitis (OM) in symptoms and panoramic radiographs. The present study aimed to investigate the possibility of detecting OS-induced trabecular bone changes and differentiating them from OM on panoramic radiographs by analyzing fractal dimensions (FDs) and degrees of anisotropy (DAs).

Materials and Methods: Panoramic radiographs of patients with histopathologically proven OS and OM of the jaw were obtained. A total of 23 patients with OS and 40 patients with OM were enrolled. To investigate whether there was a microarchitectural difference between OS lesions and normal trabecular areas in each patient, two regions of interest were located: one including the center of OS lesions and the other in the corresponding normal trabecular bone on the opposite side and to differentiate OS from OM, regions of interest were located including the center of OS and OM lesions on the CT images. Three microarchitectural parameters (box-counting FDs, fast Fourier transform-based FDs, and DAs) were calculated. A paired t-test was performed for comparison between OS lesions and normal trabecular bones, and an independent sample t-test was performed for comparison between OS and OM lesions. intraobserver and interobserver reliability of repeated measurements were calculated through intraclass correlation coefficient analysis.

Results: For both OS and OM, significant differences were found for all three microarchitectural parameters. Compared to normal trabecular bone, the trabecular bone affected by OS and OM became isotropic and more complex. When comparing OS and OM, a statistically significant difference was found only in DA. Trabecular bones affected by OS became more isotropic than those affected by OM.

Conclusion: Microarchitectural analyses, including FD and DA, would be useful in detecting tumor-induced trabecular alterations on panoramic radiographs and especially DA, could be useful for differentiating OS from OM.

Keywords: osteosarcoma; osteomyelitis; differentiation; microarchitectural analysis; panoramic radiographs; fractal dimension; degree of anisotropy

Student number: 2013-31206

Table of Contents

List of Tables

List of Figures

Chapter 1. Introduction

Osteosarcoma (OS) was reported to be the most common primary bone tumor and the third most common malignancy among children and adolescents [1]. OS is defined as a proliferating neoplasm that shares the histological finding of osteoid production in association with malignant mesenchymal cells and commonly develop in the long bones of the extremities near the metaphyseal growth plate. The incidence rates of OS were 4.0 per year per million persons. The most common site was the femur (42%), followed by the tibia (19%), humerus (10%) and the skull and jaw region (8%). OS has a bipolar age distribution, with the first peak occurring in adolescence and the second peak occurring in adults over 65 years of age. The first peak indicates a close relationship between the rapid growth phase and OS, and the second peak is likely related to Paget's disease. This tumor is aggressive locally and tends to produce early and lethal systemic metastasis [1, 2].

OS occurring in the jaw bone has a slightly different tendency from OS occurring in the long bone. Patients who develop OS in the jaw bone are generally older than those who develop in the long bones, and the rate of metastasis is lower. As a result, OS arising from the jaw bone has a better prognosis, but the 5-year survival rate is still low.

To date, the main treatment for OS is surgical resection with adjuvant chemotherapy. It has been reported that the current five-year survival rate is less than 30% for people with metastatic disease, while those with nonmetastatic disease experience survival rates exceeding 70%. [3-5]. Detecting OS before metastasis is critical to reducing surgical resection and improving five-year survival rate. However, diagnosing OS is very challenging due to its low incidence and the nonspecificity of its symptoms at presentation [6]. OS patients of jaws are usually reported to a dentist. OS of jaws frequently misdiagnosed as periapical lesions, odontogenic lesions, impactions or osteomyelitis (OM), which is an infection of the bone due to non-specific symptoms such as swelling, pain, tooth mobility and paresthesia [7, 8]. The features of OS and OM are similar on imaging and there are numerous reports of OS being misdiagnosed as OM [9-13].

Panoramic radiographs are basically used to take images of patients in dental clinics. With the advent of CBCT, more specific images can be obtained, but panoramic radiographs are still the most preferred for reasons such as low radiation dose. Therefore, panoramic radiographs could be considered as a screening tool for detection of bone malignancies, such as OS. Bone mass and microstructure have been used as useful factors for predicting bone mechanical strength [14–16]. Microarchitectural analysis on panoramic radiographs has been used to assess patients with diseases related to bone metabolism, and fractal analysis of the trabecular bone texture was performed in most of these studies [17–21]. The fractal dimension (FD) represents the complexity of the trabecular structure. Measurement of the FD in panoramic radiographs has been applied in various fields, including peri-implant bone assessment, mandibular bone-healing after orthognathic surgery, and trabecular alterations in medication-related osteonecrosis of the jaw [22–25].

Anisotropy is also an important imaging parameter for microarchitecture analysis along with fractal dimension. An anisotropy evaluation is useful for characterizing the degree of directional organization of the trabecular bone. The degree of anisotropy (DA) represents the degree of trabecular polarization in a particular direction. Several types of bones have been evaluated already for anisotropy, including the hip, calcaneus, vertebrae, and radius [26–28]. DA were examined in several studies. Osteoporotic patients presented a higher DA than controls [29]. It was difficult for computer-based automatic classification of trabecular bone pattern by DA analysis [30]. To evaluate trabecular bone quality at the implant site, DA was analyzed using cone-beam CT and micro

CT. In the study, the DA correlation between cone-beam CT and micro CT was investigated and DA parameters showed the highest agreement between cone-beam CT and micro CT [31]. Condylar internal trabecular bone structure has also been investigated and DA through cone-beam CT was found to be a reliable biomarker that can be utilized clinically. [32].

Despite the recent application of microarchitectural analysis of trabecular bone in the jaw, neither FD nor DA has been used to detect bone malignancies of the jaw. A correct diagnosis of OS is vital and its differentiation from OM is very challenging based on clinical and imaging features. There has been no study, however, on the microarchitectural analysis of panoramic radiographs for detecting and differentiating OS from OM. We hypothesized that the OS-induced trabecular microarchitecture is different from the normal trabecular architecture and that the OS-induced trabecular microarchitecture is also different from the OM-induced trabecular microarchitecture. The present study aimed to investigate the possibility of detecting OS-induced trabecular bone changes and differentiating them from OM on panoramic radiographs by analyzing FD and DA.

Chapter 2. Literature Review

1. The importance of early diagnosis of OS

Overall, treatment with preoperative chemotherapy followed by surgery and adjuvant therapy has significantly improved the survival rate of OS patients over the past few decades. However, OS still has a low five-year survival rate and is known to cause metastasis very well.

Kager et al. [4] reported that the number of metastases at diagnosis and the completeness of surgical resection of tumor sites have independent prognostic value in OS patients. Meyers et al. [3] treated 62 patients who had OS with metastasis detected at initial presentation and survival was so poor that only less than 20% of the patients survived. They stated that OS that presented with metastatic disease has a poor prognosis with therapy, although therapy has achieved good results for patients without metastasis detected at diagnosis.

In summary, the survival rate of OS patients differs greatly depending on whether they have metastatic disease, and if detected before metastasis, the survival rate can be greatly improved.

2. The importance of differential diagnosis between OS and OM

Although OS is a deadly malignant tumor with a low survival rate, it is still often misdiagnosed as other diseases such as OM and the appropriate treatment time is missed.

OS appears radiographically as osteoblastic, osteolytic and mixed lesion. The boundary of the OS lesion is unclear, and widening of the periodontal ligament space of the involved teeth might be seen. OM also has a pattern of an osteolytic and osteoblastic bone formation and the periodontal ligament space of the adjacent tooth is widened. Sequestrum could be observed but this is characteristic of chronic OM. Because the radiographic features of the two diseases are similar, it is easy to confuse OS with OM, an inflammatory disease, in the early stages of onset.

Widhe et al. [6] stated that OS was very difficult to diagnose correctly because the incidence rate was low and the symptoms were non-specific. Al-Chalabi et al. [9] reported a case in which OS was misdiagnosed because its clinical symptoms were similar to those of OM. They mentioned most common signs of bone cancer were localized pain with overlying tenderness. These signs and symptoms could be mistaken for common musculoskeletal injuries.

There have been many reports of OS that occurred in the jaw bone being misdiagnosed as OM. Karburge et al. [11] also reported a case of OS in the mandible that was misdiagnosed as an inflammatory disease due to the symptoms such as swelling, paresthesia, tenderness, and tooth mobility. ElKordy et al. [8] investigated 21 cases of OS of the jaw and announced OS was difficult to diagnose properly because there was rare specific imaging feature.

In summary, OS is often misdiagnosed as OM, an inflammatory disease, and the appropriate treatment time is often missed. This makes the prognosis significantly worse.

3. Applications of bone microarchitectural analysis on panoramic radiographs.

Bone microarchitectural analysis is being used in various field in dentistry. In particular, FD and DA have been actively used in disease research.

Using fractal analysis, Sindeaux et al. [17] analyzed 133 dental panoramic radiographs from men aged >60 years and postmenopausal women. The FD values on mandibular cortical bone were lower in women with osteoporosis.

Apolinário et al. [18] stated that children with osteogenesis imperfecta had deformed cortical bone after pamidronate treatment, resulting in higher FD of cortical bone, so FD should be considered before treatment.

Göller Bulut et al. [19] investigated 34 patients using aromatase inhibitors and found mean FD values were slightly but not significantly lower in patient's group. They mentioned that evaluation of FD on panoramic radiography could be used to determine the effect of this drug on the jaw bone.

Kış et al. [22] evaluated the peri-implant bone trabecular microstructure changes in short implant with fractal analysis. The mean FD values of the success group were significantly higher than those of the failure group. They concluded that clinically, the survival of implant could be predicted by analyzing the FD of the surrounding trabecular bone of the implant.

Heo et al. [23] evaluated the radiographic changes to the operational sites after orthognathic surgery. They stated that the FD decreased immediately after the operation, gradually increased over time, and after one year it became similar to the pre-operative level. This result suggested that FD could be used to evaluate the bony healing process after orthognathic surgery.

Chappard et al. [29] investigated 39 postmenopausal women with vertebral fracture and 70 age-matched control cases. DA evaluation from Fast Fourier Transform on bone radiographs was conducted. Vertebral fractures showed higher DA than the control group. they considered that osteoporosis was characterized by a preferential loss of trabeculae having the less mechanical competence.

Kulah et al. [31] evaluated maxillary trabecular microstructure as an indicator of implant stability by using cone beam computed tomography and micro-computed tomography. DA parameter showed the highest agreement between cone beam computed tomography and micro−computed tomography devices. They concluded DA parameters measured in CBCT were found to be useful evaluation of maxillary trabecular microstructure.

Cole et al. [33] reported micro−computed tomography derived anisotropy could detects tumor−induced deviations in bone in a murine model of orthotopic OS. They injected OS cells into the tibia in a murine model and evaluated the DA. Bone destruction areas showed decreased DA due to loss of organized bone and deposition of reactive woven bone. By analyzing the DA obtained from micro−CT, they concluded that altered bone changes due to OS could be detected.

Chapter 3. Material and Methods

This retrospective study was approved by the Institutional Review Board of the Seoul National University Dental Hospital (IRB066/03-22), and the need for informed consent was waived. All methods were performed in accordance with the relevant guidelines and regulations.

3.1. Patients

Digital panoramic radiographs of patients with histopathologically proven OS of the jaw from January 2000 to December 2020 and OM of the jaw from 2015 to 2020 were obtained from the picture archiving and communicating system at Seoul National University Dental Hospital. Patients who had a history of taking antiresorptive or antiangiogenic agents and who received radiotherapy or chemotherapy before the panoramic radiograph were taken were excluded. Patients with intramedullary OS were included, while those with surface OS were excluded. For comparisons between OS lesions and normal control areas in the same jaw, the patients with OS lesions in the anterior region of the jaw, with no corresponding normal control area on the opposite side, were also excluded. Accordingly, patients with OM lesions in the anterior region of the jaw were excluded from comparisons between OS and OM. General demographic information, including age and sex, was collected from electronic dental records.

3.2. Panoramic radiographs

All of the panoramic radiographs were acquired using the same digital panoramic machine (OP100, Instrumentarium Corp., Tuusula, Finland) at 66–73 kVp, 6.4–12 mA, and with an exposure time of 16.8–17.6 s. Patients were positioned in the panoramic machine according to the manufacturer's recommendations; the vertical line produced by the machine was aligned with the patient's sagittal plane, and the Frankfort horizontal plane was parallel to the floor. All images were obtained using PSP image plates (12 × 10 inches) and read by an FCR system (Fuji Computed Radiography 5000R, Fuji Photo Film Co. Ltd., Düsseldorf, Germany). Images were subsequently stored in a BMP format with a matrix of 1976 × 976 pixels, an image file size of 1.83 Mb, and 8-bit gray levels.

3.3. Selection of ROI

To investigate whether there was a microarchitectural difference between OS lesions and normal trabecular areas in each patient, two ROIs were located on the images: one included the center of the OS lesions and the other was in the corresponding normal trabecular bone on the opposite side (Figure 1). Both bilateral ROIs were square-shaped and the same size (average size: 96.3 × 96.9 pixels, range of size: 71–127 pixels) in each panoramic radiograph, The ROIs did not include tooth roots. For measurement of FD, a box-counting method and FFT-based method were used. For measurement of DA, directional FD was utilized [34]. Three microarchitectural parameters of box-counting FD, FFT-based FD, and DA in the two bilateral ROIs were analyzed and compared.

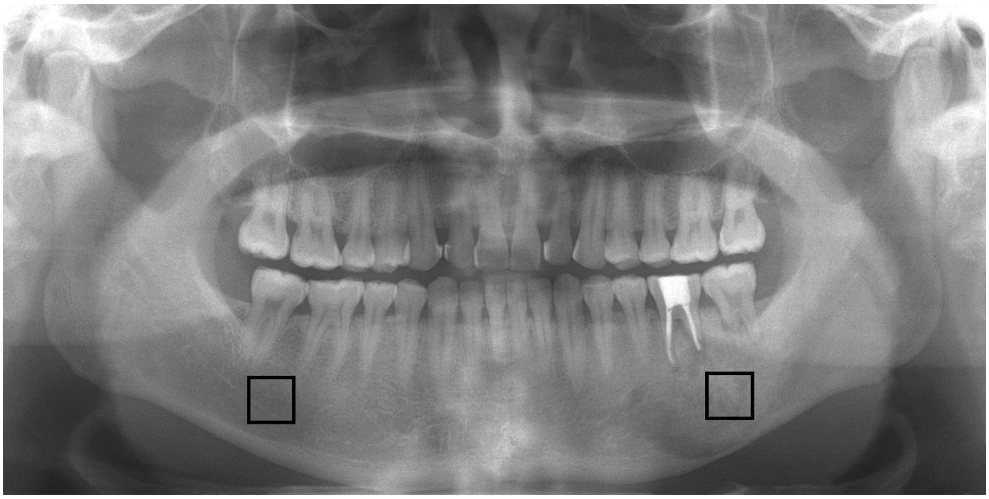

Figure 1. Panoramic radiograph of a 48-year-old man with osteosarcoma on the left mandible

Note the location of the two square regions of interest (ROIs): one ROI at the center of the osteosarcoma on the left mandibular body and the other ROI in the corresponding normal trabecular bone on the right mandibular body

For comparison of OS and OM lesions, ROIs were also defined in panoramic radiographs of OM patients. The ROIs of OM lesions were square–shaped (average size: 89.5-91.0) and did not include tooth roots. They were localized in a representative area, mostly at the epicenter of the lesion (Figure 2). To identify the representative epicenter of a lesion, CT images were used as an aid. To investigate whether there was a microarchitectural difference in normal trabecular areas between OS and OM groups, ROIs were placed bilaterally in panoramic radiographs of OM patients as well. Box–counting FD, FFT–based FD, and DA of the OM lesions were analyzed and compared with those of the OS lesions.

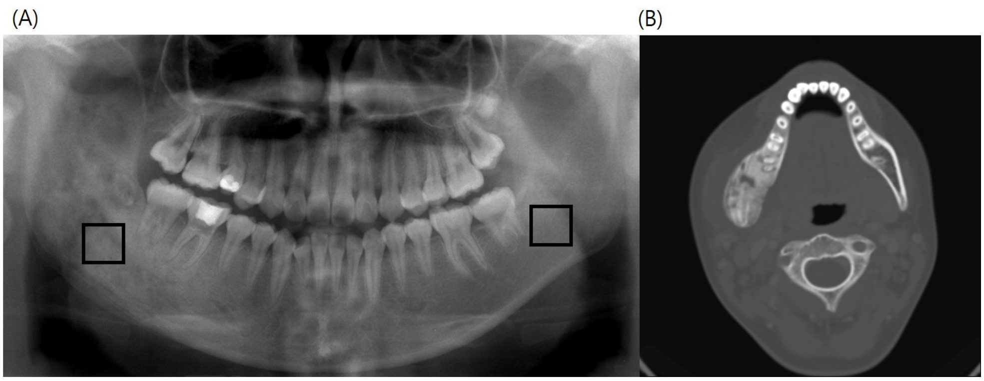

Figure 2. Panoramic radiograph of a 30–year–old woman with osteomyelitis on the right mandible

(A) A regions of interest (ROIs) was located at the center, or the representative area, of the lesion on a panoramic radiograph with reference to the corresponding CT image. The other ROI was placed in the corresponding normal trabecular bone on the left mandibular body. (B) CT image shows the osteomyelitis lesion of the right posterior mandible more clearly.

3.4. Calculation of box-counting FD

ImageJ (ver.1.52p National Institute of Health, Bethesda, MD, USA) was used to calculate the box-counting FD, which has been a traditional microarchitectural analysis method with two-dimensional (2D) radiographs. Figure 3 shows the procedure for making skeletonized images from a panoramic radiograph. All ROIs were processed using the method reported by White and Rudulph [35]. Briefly, the transferred ROI was filtered using Gaussian blur (sigma 5) to remove the fine and medium scale variations in the image brightness and then saved. The blurred image was then subtracted from the original image, and a gray value of 128 was added. The image was then made binary by threshold at a gray value of 128. The resultant image was eroded and dilated to reduce high-frequency noise. The binary image was outlined and skeletonized. The skeletonized image was used for the calculation of box-counting FD. The widths of the boxes were 2–64 pixels. All digital manipulations and measurements were made within the ROIs.

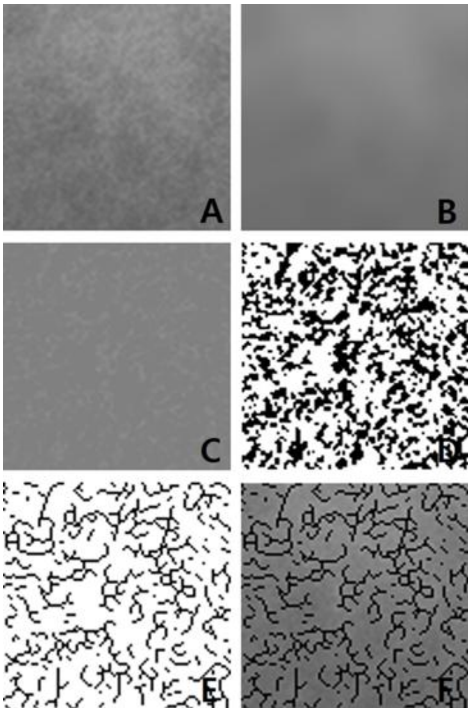

Figure 3. Digital analysis of the trabecular bone morphology

(A) A region of interest of the trabecular bone located in the center of the osteosarcoma area on the left posterior mandible in a patient' s panoramic radiograph in Figure 1. (B) Result after blurring this region. (C) Result after subtracting (B) from (A) and adding 128 (D) binary versions of the image (C). (E) The trabecular pattern is skeletonized. (F) Addition of images (A) and (E) to visually demonstrate that the skeletonized image corresponds to the original trabeculae.

3.5. Determination of FFT-based FD and DA

The process for calculating the FFT-based FD and DA was carried out in MATLAB R2020a (MathWorks, Natick, Massachusetts, USA) [34, 36]. The FFT-based technique was used for calculating the FDs of the 2D radiographs previously [34, 37-39]. The power spectrum of a local region was converted into the polar coordinate system. The FD was calculated from a curve determined by taking the logarithm of the spectrum versus the logarithm of the frequency. The directional FDs were calculated as a function of orientation based on the Fourier slice theorem (or central slice theorem), which states that the values of a one-dimensional Fourier transform of a parallel projection of an image along a line with the direction were identical to the data along the same line in the 2D Fourier transform of the image [34].

The polar plot of FDs was constructed by the directional FDs calculated in the directions 0 to 180 degrees. The plot described the moment of inertia of an object as a function of its orientation. To quantify the structural anisotropy of the trabecular bone, the major and minor principal axis directions of inertia were determined by geometrical moments calculated from the polar plot of FDs. The anisotropy was quantified as the ratio of the major and minor axes of the best-fitting ellipse [34].

In the program, as the measured DA number approached 1, the DA value decreased, and as the measured DA number approached 0, the DA value increased. This meant that the higher the measured DA number, the lower the DA value and the more isotropic the trabecular microarchitecture (Figure 4).

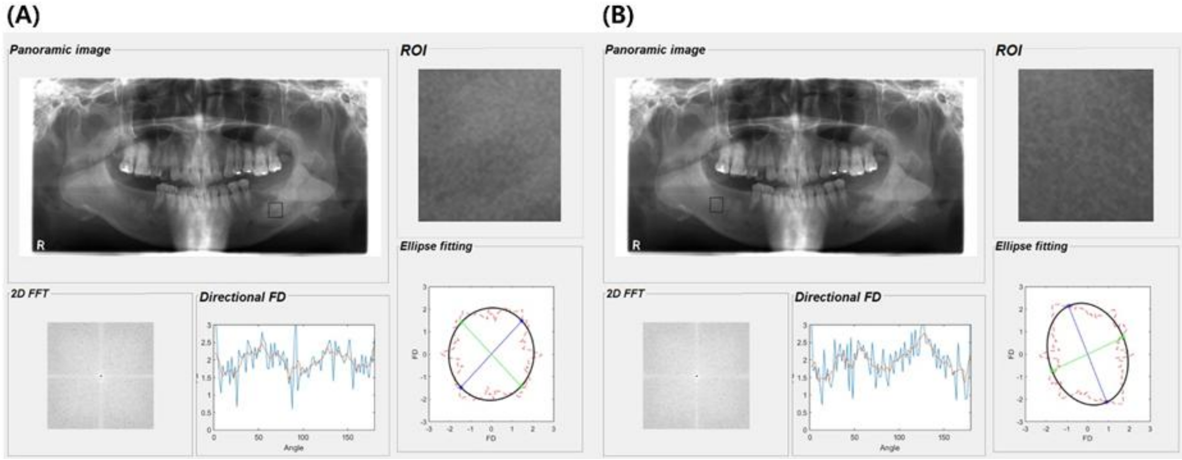

Figure 4. An example of the fast Fourier transform (FFT)−based method of calculating the fractal dimensions and degree of anisotropy (DA) of a panoramic radiograph from patients with osteosarcoma (OS) The DA of the region of interest in the OS (A) on the left mandible was 0.96 and that of the normal trabecular bone (B) on the right mandible was 0.81. OS lesions demonstrated more isotropic trabecular bone structure than the normal area.

3.6. Intra and interobserver reliability

The selection of ROIs and subsequent calculations of FD and DA were performed by two oral and maxillofacial radiologists (KHH, JEK) with over 10 years of experience. Both radiologists had previously been coached with regard to the selection of the ROIs. To quantify intraobserver agreements, the main radiologist (KHH) assessed ROI selections two times with an interval of two weeks between assessments. To test interobserver reliability, another radiologist (JEK) performed the same assessment. The strength of the intraclass correlation coefficient was evaluated as follows: values less than 0.5, between 0.5 and 0.75, between 0.75 and 0.9, and greater than 0.9 are indicative of poor, moderate, good, and excellent reliability, respectively [40].

3.7. Statistical analysis

To demonstrate the reliability of the measurement process by two radiologists, intraobserver and interobserver reliability of repeated measurements were calculated through intraclass correlation coefficient analysis. The Kolmogorov–Smirnov and Shapiro–Wilk tests were conducted to confirm normal distributions of the data. To compare sex and anatomical sites between OS and OM groups, a chi-squared test was performed at a.05 significance level and age was compared with an independent sample t-test at a.05 significance level. Values of box-counting and FFT-based FD and DA between lesions and normal trabecular bone in each OS and OM group were compared using a paired t-test at a.05 significance level. Comparisons between OS and OM lesions were performed using an independent sample t-test at a.05 significance level. IBM SPSS statistics 23 (SPSS Inc., Chicago, IL, USA) was used for statistical analyses.

Chapter 4. Results

A total of 23 patients (11 female; 12 male) with OS and 40 patients (21 female; 19 male) with OM were enrolled in the present study. The mean age of the patients with OS was 46.2 years (range 13–83 years) and the mean age of patients with OM was 45.2 years (range 11–68 years). As for the site of occurrence, six patients had OS in the maxilla (26%) and 17 in the mandible (74%), and eight patients had OM (20%) in the maxilla and 32 in the mandible (80%). Comparison of age, sex, and anatomical sites between the OS and OM groups did not show any significant differences (Table 1).

The intraclass correlation coefficients indicating interobserver and intraobserver agreement are listed in Table 2. Both intraobserver and interobserver reliabilities for repeated measurements were found to range from good to excellent.

Values of box-counting and fast Fourier transform (FFT)-based FDs and DAs satisfied the normal distribution as confirmed through both the Kolmogorov–Smirnov test and the Shapiro–Wilk test. Table 3 shows comparisons between OS and OM groups for box-counting and FFT-based FDs, and DA. There was no statistically significant difference in all the three parameters when comparing the normal areas between OS and OM groups. In each OS and OM group, statistically significant differences between lesions and normal areas were found for all the three microarchitectural parameters (P < 0.05). The largest difference between OS lesions and normal areas was shown for DA. Both methods of FD showed higher values in OS lesions than in normal areas (P < 0.05). OS lesions demonstrated lower values for DA than those of normal areas (P < 0.05). Statistically significant differences between OS and OM lesions were found only for DA. OS lesions had lower values for DA than OM lesions (P < 0.05).

Figure 5 shows box plots of the microarchitectural analyses between normal areas, OS, and OM lesions altogether. For OM lesions, as well as for OS lesions, statistically significant differences from normal areas were found for all three microarchitectural parameters. Box-counting and FFT-based FDs did not show a statistically significant difference between OS and OM lesions. However, DA revealed statistically significant differences between OS and OM lesions.

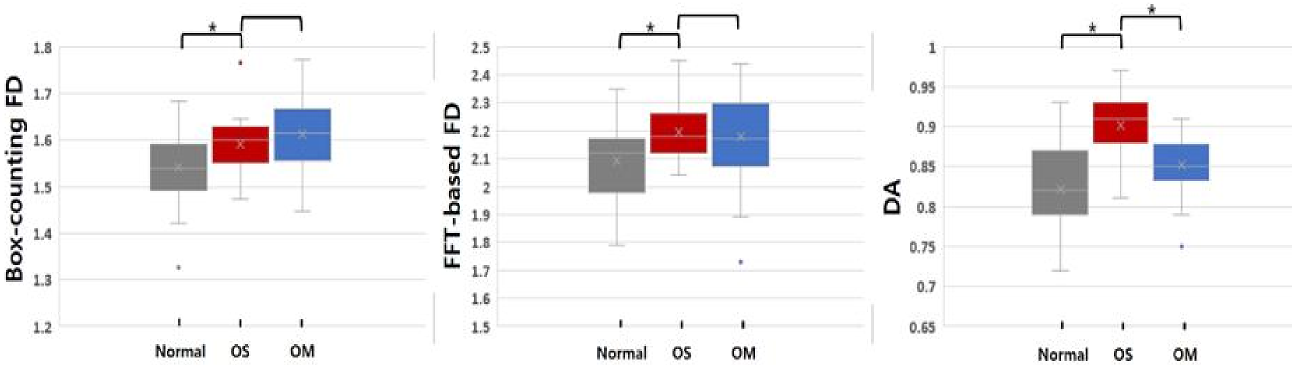

Figure 5. Box plot of the degree of anisotropy (DA), fast Fourier transform (FFT)-based fractal dimension (FD), and box-counting FD.

A paired t-test was used to compare normal areas and osteosarcoma (OS) lesions. An independent sample t-test was performed to compare OS and osteomyelitis (OM). *Significant difference ($P < 0.05$).

Table 1. Summary of the demographic characteristics and sites of occurrence of the 23 subjects with osteosarcoma and 40 subjects with osteomyelitis

Characteristic	Osteosarcoma (n = 23)	Osteomyelitis (n = 40)	P−value
Age			0.82
Mean age	46.2	45.2	
Range	13–83	11–68	
Sex, no. (%)			0.721
Female	11 (48)	21 (52.5)	
Male	12 (52)	19 (47.5)	
Site			0.754
Maxilla	6 (26)	8 (20)	
Mandible	17 (74)	32 (80)	

Age was compared using an independent sample t−test and sex and site were compared using a chi−squared test.

Table 2. Intraclass correlation coefficient analysis of bone microstructural parameters for intraobserver and interobserver agreements

	Box−counting FD				FFT−based FD				DA			
	OM lesions	OS lesions	Normal areas in OS patients	Normal areas in OM patients	OM lesions	OS lesions	Normal areas in OS patients	Normal areas in OM patients	OM lesions	OS lesions	Normal areas in OS patients	Normal areas in OM patients
Intraobserver ICC	0.864	0.808	0.762	0.780	0.915	0.892	0.758	0.923	0.856	0.801	0.897	0.805
Interobserver ICC	0.835	0.768	0.772	0.753	0.904	0.772	0.816	0.946	0.788	0.840	0.834	0.774

DA: degree of anisotropy; FD: fractal dimension; FFT: fast Fourier transform;

OS: osteosarcoma; OM: osteomyelitis

Table 3. Degree of anisotropy (DA) and fractal dimensions (FDs) between osteosarcoma (OS, n = 23) and osteomyelitis (OM, n = 40) groups (mean±standard deviation)

	Normal areas in OS patients	Normal areas in OM patients	P-value	OS lesions	OM lesions	P-value
Box-counting FD	1.541 ± 0.085	1.545 ± 0.071	0.808	1.591 ± 0.063	1.611 ± 0.076	0.276
FFT-based FD	2.093 ± 0.140	2.103 ± 0.136	0.778	2.194 ± 0.104	2.179 ± 0.168	0.674
DA	0.822 ± 0.056	0.812 ± 0.042	0.445	0.902 ± 0.042	0.852 ± 0.035	0.001*

FFT: fast Fourier transform; *: $P < 0.05$.

Chapter 5. Discussion

The present study investigated the possibility of detecting OS-induced trabecular bone changes and differentiating them from OM lesions on panoramic radiographs by analyzing the microarchitecture. Significant differences in the trabecular microarchitecture between OS lesions and normal areas were found for the three microarchitectural parameters. Of the three parameters; that is, box-counting FD, FFT-based FD, and DA, the largest difference between OS lesions and normal areas was shown for DA and only DA showed a significant difference between OS and OM lesions.

In the jaw bone, the direction of stress applied to the anterior, posterior, and condylar regions are different. Therefore, the trabecular microstructure for each region is different [34, 41]. When analyzing the microarchitectural differences between OS lesions and normal areas, the same corresponding anatomical areas of each patient were compared. One region of interest (ROI) was located at the center of OS lesions, and the other ROI was located at the corresponding normal area on the opposite side. Then, the two ROIs were compared. Using this process, we analyzed the differences in the trabecular microstructures between OS lesions and normal areas while controlling for various confounding factors such as age, sex, and anatomical sites. Comparison of age, sex, and anatomical sites between the OS and OM groups revealed no significant differences. In summary, we think that the influence of microarchitectural differences according to age, sex, and anatomical sites could be minimized when comparing OS and OM groups.

The DA is a well-known contributor to bone quality and it is a relatively independent value that has no redundant correlation with other microstructural parameters in the jaw [42]. This is the reason why the DA was considered as a candidate for being used as a microarchitectural discriminator in the present study. Although the DA is usually determined by the ratio between the maximum and minimum radii of the ellipsoid of the mean intercept length [28], the FFT-based method was used. FD was also calculated using this process in the present study. A strong correlation between these two DA analyses; that is, the mean intercept length method and the FFT-based method, was found in a previous study [34]. A low DA value means that the trabecular bones are structurally isotropic and evenly distributed without an apparent directional inclination. Our results showed that the OS lesions had lower DAs than normal areas. This means that OS lesions had a more isotropic trabecular structure. This can be thought of as the result of haphazard osteolysis and bone formation in OS. Our results also revealed that OS lesions had lower DAs than OM lesions, indicating more isotropic bone structure in OS compared to OM. In a previous study in which DAs were analyzed over time after injecting OS cells into the tibias of mice, OS lesions demonstrated a lower DA value [33], which is consistent with the results of the present study. In that previous study, micro-CT was used as an imaging modality for DA analysis, and the authors suggested that micro-CT was a complete and fairly accurate method for monitoring OS. However, micro-CT cannot be applied to humans due to radiation exposure. Instead, the possibility of applying DA analysis for the early detection of malignancies using panoramic radiographs, which are widely used in the field of dentistry, is expected to be very high.

It should be noted that in osteoporosis, the trabecular microstructure of the vertebra becomes anisotropic rather than isotropic due to a preferential loss of trabeculae with less mechanical competence [43, 44]. Since the increase or decrease in the DA value might vary depending on the kind of diseases and bones being analyzed, further studies on DA analysis using various diseases and bones are needed.

FD is widely used in the microstructural analysis of trabecular bone because FD, in addition to bone mineral density, has been shown to correlate with the biomechanical properties of bone. However, FD might be influenced by many factors, such as noise produced during the imaging process [37, 45] and the method used, so studies analyzing FD should be designed carefully [38]. On the other hand, FDs are known to be insensitive to small variations in x-ray exposure, beam alignment, and the ROI position [46, 47]. In the present study, to obtain more reliable results, FD values were calculated using two different methods (box-counting and FFT-based FD). Both methods showed significantly higher values in OS lesions than in normal areas. This means that the complexity of trabecular bone was increased in OS. Other studies using FD analysis revealed that FD was decreased immediately after orthognathic surgery and increased gradually over time [23] and that FD values of the implant success group were significantly higher than those of the failure group [22]. Like the bone-healing process in orthognathic surgery and implant osseointegration, pathological bone-forming diseases, such as OS and OM, demonstrated an increase in FD values in the present study. However, the present study showed no significant differences in FD values in the comparison between OS and OM. Therefore, it is not be possible to differentiate OS from OM with FD analysis.

With the increasing prevalence of fragility fractures due to osteoporosis, it is vital to diagnose osteoporosis early to prevent this condition. Therefore, many studies have analyzed bone microstructures. On the other hand, studies on the analysis of bone microstructure changes caused by malignancies are rare [48, 49]. To our knowledge, the present study is the first to analyze microarchitectural bone changes caused by a malignancy on panoramic radiographs. In a study on OS that occurred in other parts of the body, including the femur, pelvis, and fibula, the rate of misdiagnosis was found to be 23%. [50]. In people over the age of 60 years, a misdiagnosis rate of 43% was found due to atypical radiological findings in combination with longer time-lapses from the onset of the first symptoms to the definitive diagnosis [51]. Considering the higher rate of misdiagnosis upon initial presentation [11-13], we suggest that microarchitectural analysis using panoramic radiographs can help facilitate the early diagnosis of bone-forming sarcomas, such as OS.

The present study has some limitations. First, image noise, which might affect the microarchitectural analysis, is inherent in panoramic radiography. However, in many other studies, microstructural analysis of trabecular bone using panoramic radiographs has been performed successfully and its effectiveness has been proven. We think that image processing with Gaussian blur, erosion, and dilation would be enough to minimize the effects of image noise. Second, OS often occurs as one of three types: osteoblastic, chondroblastic, and fibroblastic. The possibility of different trabecular microstructures according to the OS type was not considered and controlled for in the present study due to the small number of patients with OS. Third, the values of the microarchitectural parameters, such as FD and DA, may vary depending on size of the ROI and where the ROI is placed within a lesion. The effect of ROI size on microarchitectural analysis using the jaw bone has yet to be studied. The periphery of OS and OM lesions might show a different microstructure from the center of the lesion. We considered the lesion's center as the area reflecting the characteristics of the lesion, and ROIs were located at the center of the lesions with reference to the CT image. The reliability of the methods in the present study was also tested. Intraobserver and interobserver agreement was found, which demonstrated good to excellent reproducibility.

The microstructural changes observed in the panoramic radiographs of the jaw bone of patients with OS were assessed. The trabecular bone affected by OS became isotropic and more complex compared to normal areas. In addition, the comparison between OS and OM showed more isotropic trabecular changes with OS and similar complexity. Microarchitectural analysis, especially DAs, could be useful in detecting OS-induced trabecular alterations and differentiating OS from OM on panoramic radiographs, which are widely used as an imaging modality in dental clinics.

Chapter 6. Conclusion

Microstructural analysis, including FD and DA, is useful for detecting tumor−induced trabecular alterations on panoramic radiographs, and DA in particular can be useful for differentiating OS from OM.

Published papers related to this study

Jung J-H, Huh K-H, Yong T-H, Kang J-H, Kim J-E, Yi W-J, Heo M-S and LEE S-S. Differentiation of osteosarcoma from osteomyelitis using microarchitectural analysis on panoramic radiographs. Sci Rep 12, 12339 (2022). https://doi.org/10.1038/s41598-022-16504-9

References

1. Ottaviani G, Jaffe N. The epidemiology of osteosarcoma. Cancer Treat Res 2009; 152: 3-13.

2. Raymond AK, Jaffe N. Osteosarcoma multidisciplinary approach to the management from the pathologist's perspective. Cancer Treat Res 2009; 152: 63-84.

3. Meyers PA, Heller G, Healey JH, Huvos A, Applewhite A, Sun M, et al. Osteogenic sarcoma with clinically detectable metastasis at initial presentation. J Clin Oncol 1993; 11: 449-53.

4. Kager L, Zoubek A, Pötschger U, Kastner U, Flege S, Kempf-Bielack B, et al. Primary metastatic osteosarcoma: presentation and outcome of patients treated on neoadjuvant cooperative osteosarcoma study group protocols. J Clin Oncol 2003 15; 2011-8.

5. Mirabello L, Troisi RJ, Savage SA. Osteosarcoma incidence and survival rates from 1973 to 2004: data from the Surveillance, Epidemiology, and End Results Program Cancer 2009; 115: 1531-43.

6. Widhe B, Widhe T. Initial symptoms and clinical features in osteosarcoma and Ewing sarcoma. J Bone Joint Surg Am 2000; 82: 667-74.

7. Arora P, Rehman F, Girish KL, Kalra M. Osteosarcoma of mandible: detailed radiographic assessment of a case. Contemp Clin Dent 2013; 4: 382-5.

8. ElKordy MA, ElBaradie TS, ElSebai HI, KhairAlla SM, Amin AAE. Osteosarcoma of the jaw: challenges in the diagnosis and treatment. J Egypt Natl Canc Inst 2018; 30: 7-11.

9. Al-Chalabi MM, Jamil I, Wan Sulaiman WA. Unusual location of bone tumor easily misdiagnosed: distal radius osteosarcoma treated as osteomyelitis. Cureus 2021; 13: e19905.

10. Bracamonte JD, Roberts CC. Chronic recurrent multifocal osteomyelitis mimicking osteosarcoma. Radiol Case Rep 2015; 1: 42-6.

11. Kalburge JV, Sahuji SK, Kalburge V, Kini Y. Osteosarcoma of mandible. J Clin Diagn Res 2012; 6: 1597-9.

12. Huvos AG. Bone Tumors: Diagnosis, Treatment and Prognosis. 1987.

13. Petrikowski CG, Pharoah MJ, Lee L, Grace MG. Radiographic differentiation of osteogenic sarcoma, osteomyelitis, and fibrous dysplasia of the jaws. Oral Surg Oral Med Oral Pathol Oral Radiol Endod 1995; 80: 744-50.

14. Pothuaud L, Van Rietbergen B, Mosekilde L, Beuf O, Levitz P, Benhamou CL, et al. Combination of topological parameters and

bone volume fraction better predicts the mechanical properties of trabecular bone. J Biomech 2002; 35: 1091–9.

15. Thomsen JS, Ebbesen EN, Mosekilde LI. Relationships between static histomorphometry and bone strength measurements in human iliac crest bone biopsies. Bone. 1998; 22: 153–63.

16. Borah B, Dufresne TE, Cockman MD, Gross GJ, Sod EW, Myers WR, et al. Evaluation of changes in trabecular bone architecture and mechanical properties of minipig vertebrae by three-dimensional magnetic resonance microimaging and finite element modeling. J Bone Miner Res 2000; 15: 1786–97.

17. Sindeaux R, Figueiredo PT, de Melo NS, Guimarães AT, Lazarte L, Pereira FB, et al. Fractal dimension and mandibular cortical width in normal and osteoporotic men and women. Maturitas 2014; 77: 142–8.

18. Apolinário AC, Sindeaux R, de Souza Figueiredo PT, Guimarães AT, Acevedo AC, Castro LC, et al. Dental panoramic indices and fractal dimension measurements in osteogenesis imperfecta children under pamidronate treatment. Dentomaxillofac Radiol. 2016; 45: 20150400.

19. Göller Bulut D, Bayrak S, Uyeturk U, Ankarali H. Mandibular indexes and fractal properties on the panoramic radiographs of the patients using aromatase inhibitors. Br J Radiol 2018; 91: 20180442.

20. Kavitha MS, An SY, An CH, Huh KH, Yi WJ, Heo MS, et al. Texture analysis of mandibular cortical bone on digital dental panoramic radiographs for the diagnosis of osteoporosis in Korean women. Oral Surg Oral Med Oral Pathol Oral Radiol 2015; 119: 346-56.

21. Pothuaud L, Lespessailles E, Harba R, Jennane R, Royant V, Eynard E, et al. Fractal analysis of trabecular bone texture on radiographs: discriminant value in postmenopausal osteoporosis. Osteoporos Int 1998; 8: 618-25.

22. Kış HC, Güleryüz Gürbulak A. Evaluation of the peri-implant bone trabecular microstructure changes in short implants with fractal analysis. Int J Implant Dent 2020; 6: 13.

23. Heo MS, Park KS, Lee SS, Choi SC, Koak JY, Heo SJ, et al. Fractal analysis of mandibular bony healing after orthognathic surgery. Oral Surg Oral Med Oral Pathol Oral Radiol Endod 2002; 94: 763-7.

24. Şahin O, Odabaşı O, Demiralp KÖ, Kurşun-Çakmak EŞ, Aliyev T. Comparison of findings of radiographic and fractal dimension analyses on panoramic radiographs of patients with early-stage and advanced-stage medication-related osteonecrosis of the jaw. Oral Surg Oral Med Oral Pathol Oral Radiol 2019; 128: 78-86.

25. Kato CN, Barra SG, Pereira MJ, Gomes LT, Amaral TM, Abreu LG, et al. Mandibular radiomorphometric parameters of women with cemento−osseous dysplasia. Dentomaxillofac Radiol 2020; 49: 20190359.

26. Mosekilde L, Viidik A, Mosekilde, L. Correlation between the compressive strength of iliac and vertebral trabecular bone in normal individuals. Bone 1985; 6: 291−5.

27. Geraets WG, Van der Stelt PF, Netelenbos CJ, Elders PJ. A new method for automatic recognition of the trabecular pattern. J Bone Miner Res. 1990; 5: 227−33.

28. Majumdar S, Kothari M, Augat P, Newitt DC, Link TM, Lin JC, et al. High−resolution magnetic resonance imaging: three−dimensional trabecular bone architecture and biochemical properties. Bone 1998; 22: 445−54.

29. Chappard C, Brunet−Imbault B, Lemineur G, Giraudeau B, Basillais A, Harba R, et al. Anisotropy changes in post−menopausal osteoporosis: characterization by a new index applied to trabecular bone radiographic images. Osteoporos Int 2005; 16: 1193−202.

30. Nicolielo LF, Van Dessel J, van Lenthe GH, Lambrichts I, Jacobs R. Computer−based automatic classification of trabecular bone pattern can assist radiographic bone quality assessment at dental implant site. Br J Radiol 2018; 91: 20180437.

31. Kulah K, Gulsahi A, Kamburoğlu K, Geneci F, Ocak M, Celik HH, et al. Evaluation of maxillary trabecular microstructure as an indicator of implant stability by using 2 cone beam computed tomography systems and micro-computed tomography. Oral Surg Oral Med Oral Pathol Oral Radiol 2019; 127: 247-56.

32. Ebrahim FH, Ruellas AC, Paniagua B, Benavides E, Jepsen K, Wolford L, et al. Accuracy of biomarkers obtained from cone beam computed tomography in assessing the internal trabecular structure of the mandibular condyle. Oral Surg Oral Med Oral Pathol Oral Radiol 2017; 124: 588-99.

33. Cole HA, Ohba T, Ichikawa J, Nyman JS, Cates JM, Haro H, et al. Micro-computed tomography derived anisotropy detects tumor provoked deviations in bone in an orthotopic osteosarcoma murine model. PLoS One 2014; 9: e97381.

34. Yi WJ, Heo MS, Lee SS, Choi SC, Huh KH, Lee SP. Direct measurement of trabecular bone anisotropy using directional fractal dimension and principal axes of inertia. Oral Surg Oral Med Oral Pathol Oral Radiol Endod 2007; 104: 110-6.

35. White SC, Cohen JM, Mourshed FA. Digital analysis of trabecular pattern in jaws of patients with sickle cell anemia. Dentomaxillofac Radiol 2000; 29: 119-24.

36. Miras, J. Fractal Analysis in MATLAB: A Tutorial for

Neuroscientists. In: Di Ieva, A. (eds) The Fractal Geometry of the Brain. Springer Series in Computational Neuroscience. Springer New York, NY. p. 523–32

37. Geraets WG, van der Stelt PF. Fractal properties of bone. Dentomaxillofac Radiol 2000; 29: 144–53.

38. Majumdar S, Lin J, Link T, Millard J, Augat P, Ouyang X, et, al. Fractal analysis of radiographs: assessment of trabecular bone structure and prediction of elastic modulus and strength. Med Phys 1999; 26: 1330–40.

39. Millard J, Augat P, Link TM, Kothari M, Newitt DC, Genant HK, et al. Power spectral analysis of vertebral trabecular bone structure from radiographs: orientation dependence and correlation with bone mineral density and mechanical properties. Calcif Tissue Int 1998; 63: 482–9.

40. Koo TK, Li MY. A Guideline of Selecting and Reporting Intraclass Correlation Coefficients for Reliability Research. J Chiropr Med 2016; 15: 155–63.

41. Kim JE, Shin JM, Oh SO, Yi WJ, Heo MS, Lee SS, et al. The three–dimensional microstructure of trabecular bone: Analysis of site–specific variation in the human jaw bone. Imaging Sci Dent. 2013; 43: 227–33.

42. Huh KH, Yi WJ, Jeon IS, Heo MS, Lee SS, Choi SC, et al.

Relationship between two-dimensional and three-dimensional bone architecture in predicting the mechanical strength of the pig mandible. Oral Surg Oral Med Oral Pathol Oral Radiol Endod 2006; 101: 363-73.

43. Brunet-Imbault B, Lemineur G, Chappard C, Harba R, Benhamou CL. A new anisotropy index on trabecular bone radiographic images using the fast Fourier transform. BMC Med Imaging 2005; 5: 4.

44. Mosekilde L. Sex differences in age-related loss of vertebral trabecular bone mass and structure-biomechanical consequences. Bone 1989; 10: 425-32.

45. Veenland JF, Grashuis JL, Gelsema ES. Texture analysis in radiographs: the influence of modulation transfer function and noise on the discriminative ability of texture features. Med Phys 1998; 25: 922-36.

46. Samarabandu J, Acharya R, Hausmann E, Allen K. Analysis of bone X-rays using morphological fractals. IEEE Trans Med Imaging 1993; 12: 466-70.

47. Shrout MK, Potter BJ, Hildebolt CF. The effect of image variations on fractal dimension calculations. Oral Surg Oral Med Oral Pathol Oral Radiol Endod 1997; 84: 96-100.

48. Tamada T, Sone T, Jo Y, Imai S, Kajihara Y, Fukunaga M.

Three−dimensional trabecular bone architecture of the lumbar spine in bone metastasis from prostate cancer: comparison with degenerative sclerosis. Skeletal Radiol 2005; 34: 149−55.

49. Bi X, Sterling JA, Merkel AR, Perrien DS, Nyman JS, Mahadevan−Jansen A. Prostate cancer metastases alter bone mineral and matrix composition independent of effects on bone architecture in mice−−a quantitative study using microCT and Raman spectroscopy. Bone 2013; 56: 454−60.

50. Okada K, Hasegawa T, Nishida J, Ogose A, Tajino T, Osanai T, et al. Osteosarcomas after the age of 50: a clinicopathologic study of 64 cases−an experience in northern Japan. Ann Surg Oncol 2004; 11: 998−1004.

51. Sadoghi P, Leithner A, Clar H, Glehr M, Wibmer C, Bodo K, et al. The threat of misdiagnosis of primary osteosarcoma over the age of 60: a series of seven cases and review of the literature. Arch Orthop Trauma Surg 2010; 130: 1251−6.

국문초록

파노라마방사선영상에서 골육종과 골수염의 감별을 위한 프랙탈 차원과 비등방성 분석

서울대학교 대학원 치의과학과 영상치의학 전공

(지도교수 허 경 회)

정 지 훈

1. 목 적

악성 병소인 골육종을 치과에서 초기에 진단하는 것은 매우 어려운 일이며, 골육종은 임상 증상과 파노라마 방사선영상에서 염증성 병소인 골수염과 유사하게 보이기 때문에 오진하기 쉽다. 본 연구에서는 파노라마 방사선영상에서 해면골 미세구조 분석(프랙탈 차원, 비등방성)을 이용하여 골육종에 의한 해면골 변화를 감지하고 골육종을 골수염과 감별할 수 있는 가능성을 조사하고자 한다.

2. 방 법

조직병리학적으로 입증된 악골에서 발생한 골육종과 골수염환자의 파노라마 방사선영상과 CT 영상을 수집하였다. 2000년부터 1월 1일부터 2020년 12월 30일까지 서울대학교 치과병원에 진료목적으로 파노라마

방사선사진을 촬영하고 조직병리학적으로 입증된 골육종 환자 23명과 2015년부터 1월 1일부터 2020년 12월 30일까지 조직병리학적으로 입증된 골수염 환자 40명의 파노라마 방사선영상을 수집하였다. 각 환자에서 골육종 병소와 정상 해면골 간에 미세구조적 차이가 있는지 여부를 조사하기 위해 2개의 관심영역을 설정하였다. CT 영상을 바탕으로 골육종 병변의 중심에 관심영역을 설정하였고 반대쪽의 대칭되는 부위에 비교할 수 있는 관심영역을 설정하였다. 해면골 미세구조 분석을 위해서 3가지 매개변수 (Box-counting 프랙탈 차원, fast Fourier transform-based 프랙탈 차원, 비등방성)를 관찰하였다. 골육종 병소과 정상 소주골을 비교하기 위해 대응표본 t 검정을 시행하였고, 골육종과 골수염 병소를 비교하기 위해 독립표본 t 검정을 시행하였다. 반복 측정의 측정자간 및 측정자내 신뢰도는 급내상관계수를 통해 계산되었다.

3. 결 과

골육종과 골수염 모두에서 정상 해면골과 비교하였을 때 골 미세구조 매개변수 (Box-counting 프랙탈 차원, fast Fourier transform-based 프랙탈 차원, 비등방성) 모두에서 상당한 차이가 발견되었다. 정상적인 해면골과 비교하여 골육종과 골수염에 영향을 받은 해면골은 보다 등방성이며 프랙탈구조가 더 복잡해졌다.

골육종을 골수염과 비교했을 때 통계적으로 유의한 차이는 비등방성에서만 발견되었다. 골육종에 의해 영향을 받은 해면골은 골수염에 의해 영향을 받은 해면골보다 더욱 등방성이 되었고 프랙탈 구조는 유의미한

차이가 나지 않았다.

4. 결　론

　본 연구에서는 프랙탈 차원과 비등방성을 포함한 미세구조 분석은 파노라마 방사선영상에서 종양으로 유발된 해면골의 변화를 감지하는데 유용하며 특히 비등방성은 골육종을 골수염과 감별진단 하는데 유용하다는 것을 확인하였다.

주요어 : 골육종, 골수염, 감별진단, 골 미세구조 분석, 파노라마 방사선영상, 프랙탈 차원, 비등방성

학　번 : 2013-31206